scientific reports

Check for updates

OPEN

Correction of exon 2, exon 2–9 and exons 8–9 duplications in DMD patient myogenic cells by a single CRISPR/Cas9 system

Juliette Lemoine[1,2], Auriane Dubois[1,2], Alan Dorval[1,2,4], Abbass Jaber[1,2], Ganesh Warthi[1,2], Kamel Mamchaoui[3], Tao Wang[1,2], Guillaume Corre[1,2], Matteo Bovolenta[1,2,5,6] & Isabelle Richard[1,2,6]✉

Duchenne Muscular dystrophy (DMD), a yet-incurable X-linked recessive disorder that results in muscle wasting and loss of ambulation is due to mutations in the dystrophin gene. Exonic duplications of dystrophin gene are a common type of mutations found in DMD patients. In this study, we utilized a single guide RNA CRISPR strategy targeting intronic regions to delete the extra duplicated regions in patient myogenic cells carrying duplication of exon 2, exons 2–9, and exons 8–9 in the *DMD* gene. Immunostaining on CRISPR-corrected derived myotubes demonstrated the rescue of dystrophin protein. Subsequent RNA sequencing of the DMD cells indicated rescue of genes of dystrophin related pathways. Examination of predicted close-match off-targets evidenced no aberrant gene editing at these loci. Here, we further demonstrate the efficiency of a single guide CRISPR strategy capable of deleting multi-exon duplications in the *DMD* gene without significant off target effect. Our study contributes valuable insights into the safety and efficacy of using single guide CRISPR strategy as a potential therapeutic approach for DMD patients with duplications of variable size.

Treatment of progressive and fatal genetic diseases has been one of the biggest challenges to modern medicine. Duchenne muscular dystrophy (DMD) is one such rare genetic disorder[1,2] causing severe progressive muscle-wasting (OMIM 310,200). It is an X chromosome linked recessive disorder that affects roughly 1/5000 male births. DMD is caused by mutations such as exon deletions, exon duplications, point mutations, insertions and splice site mutations in the dystrophin (*DMD*) gene[3–5]. Two therapeutic genetic approaches for DMD have reached clinical trials: reframing by exon skipping with antisense oligonucleotides (ASO) and expression of truncated *DMD* open reading frame (ORF) called micro-dystrophins to compensate the lack of dystrophin[6–9]. This effort has led to marketing authorization of four antisense products in the US[10] and the approval of the first micro-dystrophin product Elevidys[11]. Nevertheless, efficacy of these strategies is debated. For example, ASOs mediated exon skipping approaches have shown modest increase in dystrophin expression[12–14], whereas the micro-dystrophin approach suffers from the fact that it is conceptually unable to compensate for a full-size dystrophin, modifying DMD to a less severe form called Becker muscular dystrophy[6]. In addition, adverse events were observed during the clinical trials such as hepatotoxicity, thrombotic microangiopathy, or cardiomyositis and death[15]. Therefore, it is imperative to explore and test other potential strategies to cure DMD.

According to the Leiden database (https://www.dmd.nl/), exon duplications correspond to 10–15% of all mutations that induce a frameshift in the *DMD* ORF, resulting in premature termination. Interestingly, *DMD* exon duplications offer a context where it is possible to revert to a full-length dystrophin. This was initially demonstrated with the use of ASO in a mouse model with a duplication of the exon 2[15]. Subsequently, a CRISPR/Cas9 strategy employing a single guide RNA was developed, leading to the stable removal of duplications spanning exons 18–30[16] and exon 2 in immortalized myoblasts[17], exons 55–59 in induced pluripotent stem cell (iPSC) differentiated to cardiomyocytes[18] as well as exons 18–25[19] and exons 3–16 in primary myoblasts[20]. This gene editing

[1]Genethon, 1, bis rue de l'internationale, 91000 Evry, France. [2]Université Paris-Saclay, Univ Evry, Inserm, Généthon, Integrare Research Unit UMR_S951, 91000 Evry-Courcouronnes, France. [3]Sorbonne Université, Inserm, Institut de Myologie, Centre de Recherche en Myologie, 75013 Paris, France. [4]Present address: ADLIN Science, Pépinière « Genopole Entreprises », 91058 Evry, France. [5]Present address: Department of Translational Medicine, University of Ferrara, 44121 Ferrara, Italy. [6]These authors contributed equally: Matteo Bovolenta and Isabelle Richard. ✉email: richard@genethon.fr

approach to revert duplications was further explored in a novel mouse model with an exon 18–30 duplication[21]. In this current study, we further demonstrate the potential of a single gRNA strategy to delete DMD duplications of variable size. After selection of potent guides for Streptococcus pyogenes (Sp) Cas9, CRISPR deletion of three different duplicated regions was achieved in patient immortalized myogenic cell lines without detection of off-target activity. Restored expression of the dystrophin protein was observed as well as genes of dystrophin-related pathways. This study further validates CRISPR/Cas9 as potential therapeutic option for correcting multiple exon duplications in DMD patients.

Results

Single gRNA CRISPR strategy corrects exon duplication in Dup2, Dup2–9 and Dup8-9 patient cells, restoring dystrophin ORF

Myoblasts from patients carrying duplication of exon 2 (Dup2 line), of exons 2 to 9 (Dup2–9 line), or of exons 8 and 9 (Dup8-9 line) were obtained through the Biobank of Cells, tissues and DNA from patients with neuromuscular diseases, member of the Telethon Network of Genetic Biobanks (project no. GTB12001), funded by Telethon Italy and immortalized by the Myoline platform. We verified the genotypes of these cell lines by digital droplet PCR (ddPCR) analysis (Fig. 1A). For this purpose, primers for a ddPCR assay were designed (Table S1) to quantify the copy number of the duplicated regions in treated cells, normalizing it to a non-duplicated region within intron 30 of the DMD gene. Further, we excluded the expression of residual amount of dystrophin by capillary western blot (Fig. 2C). Comparative genomic hybridization analysis (DMD-CGH[22], Fig. S1) allowed characterization of the duplications spanning from intron 1 to intron 9 in Dup2–9 cells (chrX:32673721-33180918dup) and from intron 7 to intron 9 in Dup8-9 cells (chrX:32639886-32700772dup). Dup2 cells were previously reported[17] (cells 994) and carry a duplication of 137 kb from intron 1 to intron 2 (chrX:32937559-33094577dup). All coordinates reported here and in Fig. S1 are based on GrCh37 (hg19) assembly.

To remove the duplicated regions in these DMD myoblasts (Fig. 1B), guide RNAs (gRNAs) for spCas9 were designed using the CRISPOR tool[23] and selected considering their specificity score with minimal predicted off targets (Table 1). The genomic regions used to design these gRNAs were selected based on the commonly duplicated intronic regions among patients, carefully avoiding splicing signals. Three sgRNAs were selected for testing for Dup2 and Dup2–9 lines correction and two sgRNAs for Dup8-9 line correction among the many generated by CRISPOR. The in vitro on-target cutting efficiencies of three selected sgRNAs (sgRNA1, sgRNA2 and sgRNA3) for Dup2 and Dup2–9 correction were validated via cell independent CRISPR-in-tube approach where a PCR product of target region is mixed with a ribonucleoprotein (RNP) complex followed by densitometric analysis on an Agilent 2100 bioanalyzer (Fig. 1C; Fig. S2; Table S2). The sgRNA3 showed the highest editing efficiency of 97.00%, whereas sgRNA1 and sgRNA2 showed cutting efficiency of 94.90% and 93.78%, respectively (Fig. 1C). Since the CRISPR-in-tube approach gave overestimated cutting compared to what is usually seen in a cellular context, we decided to test cutting efficiencies of the two selected sgRNAs (sgRNA-A and sgRNA-B) for Dup8-9 correction by cloning them in a spCas9-GFP coding plasmid (px458 Addgene[24]) and transfecting the constructs into HEK293 cells. Forty-eight hours after transfection, the target DNA region was PCR-amplified and sequenced for TIDE analysis (http://shinyapps.datacurators.nl/tide), revealing a higher cutting efficiency of sgRNA-A (21.75%) compared to sgRNA-B (17.15%) (Fig. 1D; Fig. S3; Table S2).

The immortalized myoblasts were nucleofected with RNP complexes comprising spCas9-GFP protein and the selected sgRNA-3 for Dup 2 and Dup 2–9, or sgRNA-A for Dup 8-9 myoblasts, aiming to correct the *DMD* ORF. Cells were sorted individually per well and cultured for forty days. In total, eleven clones were obtained for Dup2, and more than twenty clones for Dup2–8 and Dup8-9. The ddPCR analysis revealed the removal of the duplicated regions in one, five and seven clones for Dup2, Dup2–9 and Dup8-9 cells, respectively (Fig. 2A).

To validate the restoration of the *DMD* reading frame following the excision of duplicated exons, clone 7 for Dup2, clone 14 for Dup2–9, and clone 12 for Dup8-9 myoblasts were plated with differentiation media to obtain differentiation into myotubes. All three clones, 5 days post-culture in differentiation media, showed dystrophin expression as validated by immunostaining (Fig. 2B). Capillary western blot analysis confirmed dystrophin expression in myotubes, with an average expression level of 20% compared to the myotube differentiated from a wild- type (WT) immortalized myoblast cell line C25 (Fig. 2C).

RNAseq analysis indicates correction of DMD dysregulated pathways

We have successfully demonstrated that our sgRNA CRISPR strategy can correct the duplication of the *DMD* gene and restore the expression of the full protein. To better understand the consequences of restoring dystrophin at molecular level, we performed RNA sequencing using the Illumina technique on selected clones along with C25 after seven days of differentiation. The sequencing was performed in three replicates with the sequencing depth between 30 and 50 M reads per sample. The Phred Score was above 30 for all position on the single length of all samples. On average, alignment on the transcriptome GRCh38.P13 (Gencode Version 43) was 76.59%

Initially, we focused on the expression of the *DMD* gene, which showed significant repression in the uncorrected DMD cells compared to C25 cells. There was a dramatic activation of expression in the corrected clones compared to the uncorrected DMD cells, reaching approximately 70% of the expression level in the C25 cells (Fig. 3A). Then, we analysed exon usage in the *DMD* gene (Fig. 3B, Supplemental excel file 1). We divided the exons of *DMD* into three groups: Beginning, Middle and End exons. Consistent with the findings that the *DMD* gene exhibits transcription imbalance in DMD patients, we observed that the *DMD* transcript levels gradually decreased from the Beginning exons to the End exons across all the duplicated cell lines we used. However, when the *DMD* gene is successfully corrected, this transcription imbalance is also rectified.

Globally, in the RNA-seq, we observed an up-regulation of 1600, 1308 and 1248 genes and a down-regulation of 1285, 1332 and 1484 genes in the Dup2, Dup2–9 and Dup8-9 when compared to C25, respectively (Fig. S4A).

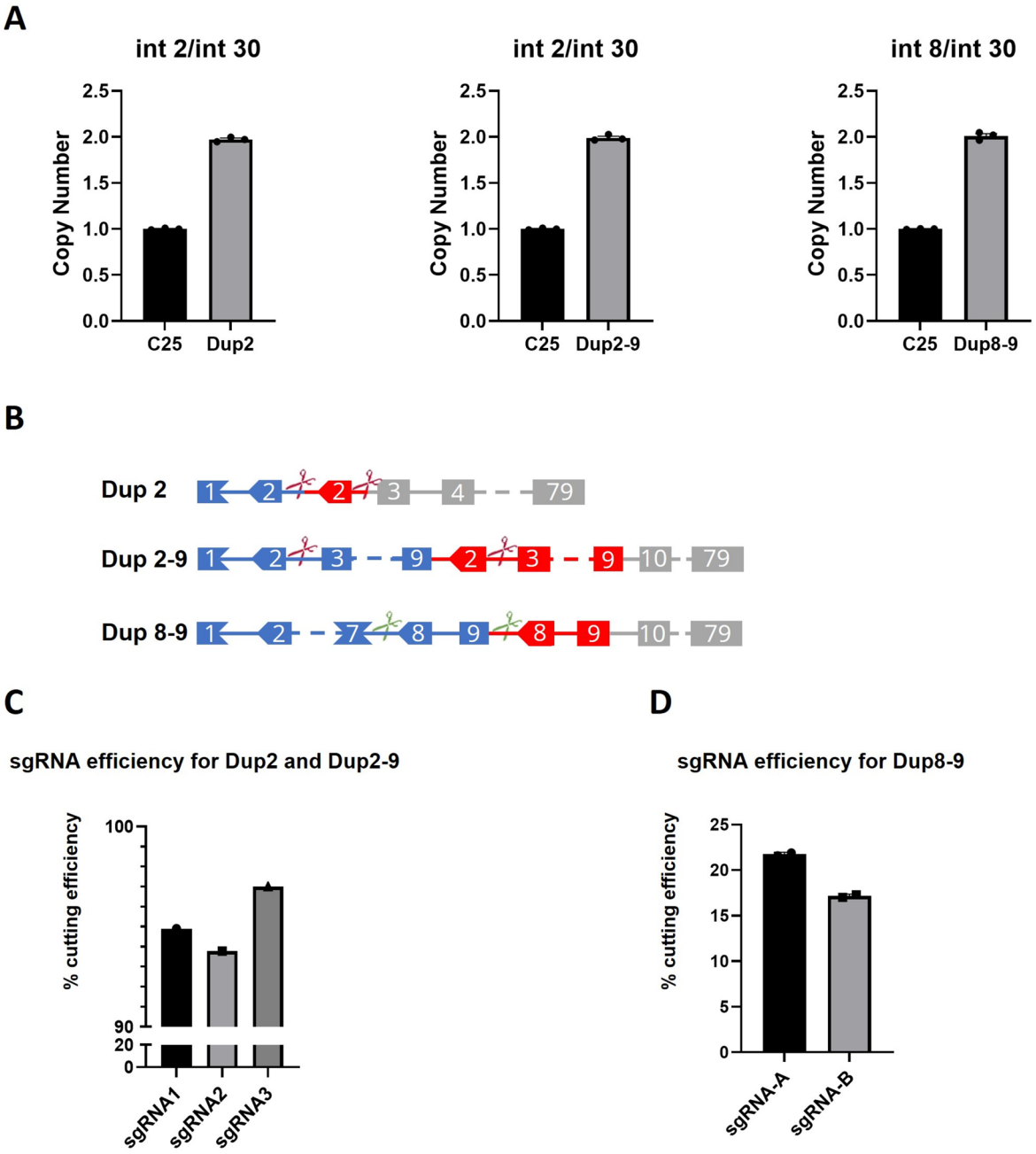

Figure 1. The single gRNA CRISPR strategy for correcting exon duplications in cells of DMD patients. (**A**) Results of the ddPCR quantification of the number of exons in DNA of the cell lines, with wild type immortalized myoblasts cell line C25 cells used as a control. (**B**) Scheme of the organization of the DMD gene in patient-derived immortalized myoblasts harboring exon duplications with location of the respective sgRNA. From top to bottom: exon 2 (Dup2), exons 2–9 (Dup2–9) and exon 8–9 (Dup8-9). (**C**) Relative cutting efficiency of the selected sgRNA for Dup2 and Dup2–9 assessed by CRISPR in-tube. (**D**) Relative cutting efficiency of the selected sgRNA for Dup8-9 assessed by TIDE analysis following transfection in HEK293 cells.

Of these genes, 520 were commonly down-regulated, and 407 were consistently up-regulated in all three uncorrected DMD cells (Fig. S5, Supplemental excel file 2). In addition, we observed an up-regulation of 594, 224 and 738 genes and a down-regulation of 822, 298 and 569 genes in the Dup2 clone 7 when compared to Dup2, Dup2–9 clone 14 when compared to Dup2–9 and Dup8-9 clone 12 when compared to Dup8-9, respectively (Fig. S4B). Data complexity reduction using principal component analysis (PCA) showed that the distance between the different cells was larger than the distance between the corrected and uncorrected cells (which are de facto isogenic to each other) (Fig. S6A). We also analyzed a publicly available dataset (GSE262976) that used a similar transcriptomics profiling technique as our study on CRISPR-corrected DMD myogenic cells derived from iPSCs[25]. This study included one WT, two DMD patient-specific iPSC cell lines carrying mutations in exons 45 and 51, and two DMD- CRISPR corrected counterparts. PCA analysis of this dataset also showed that

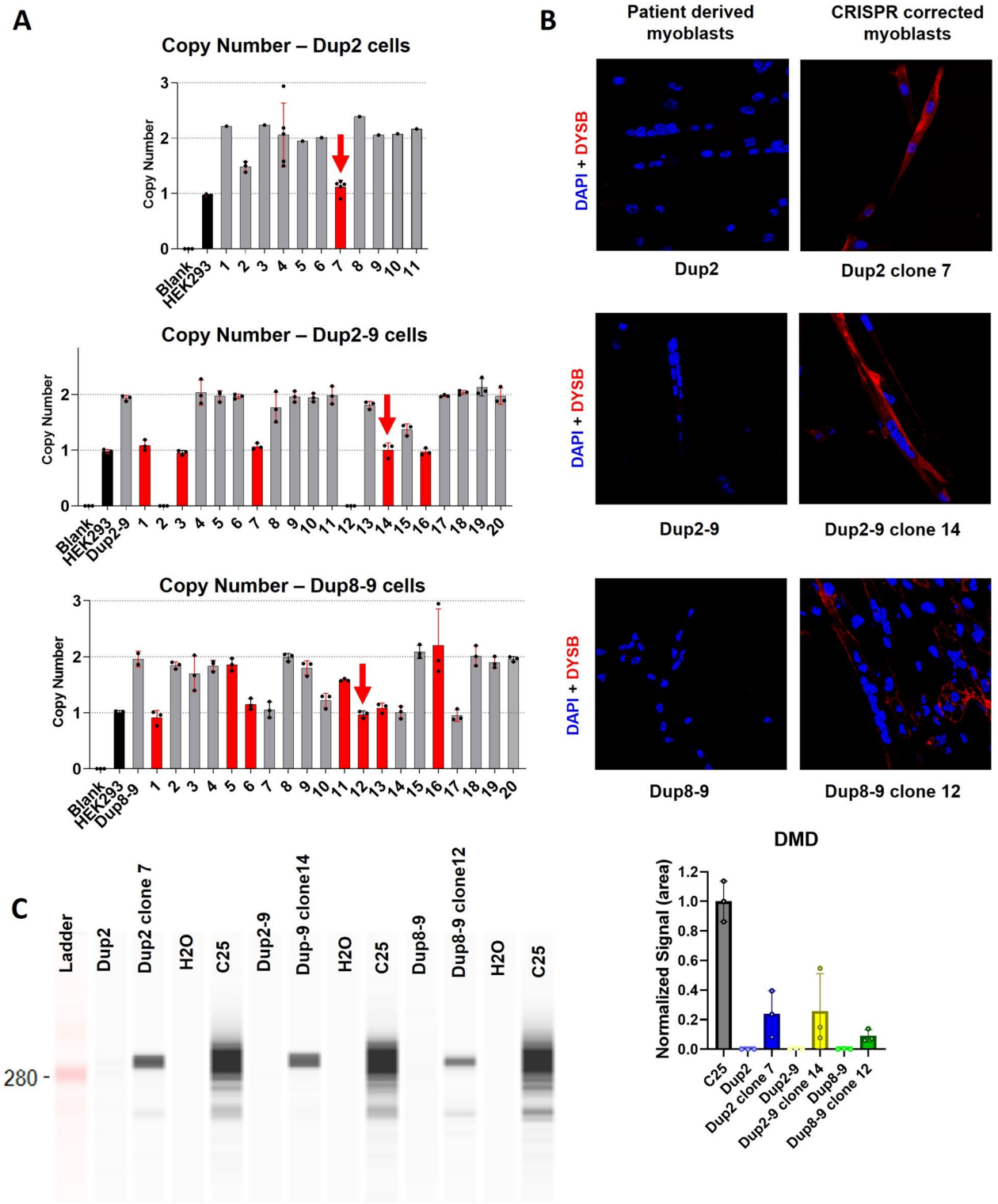

Figure 2. The single gRNA CRISPR strategy successfully corrects exon duplications in cells from DMD patients. (**A**) Results of the ddPCR for quantifying the number of exons in isolated clones following CRISPR editing. The clones where only one copy was detected are indicated in red. (**B**) Immunostaining of dystrophin by the antibody DYSB (in red) in the Dup2, Dup2–9, Dup8-9 (left panel) and Dup2 clone 7, Dup2–9 clone 14, Dup8-9 clone 12 (right panel) cell lines. Nuclei were stained with DAPI (in blue) The scale bar is 40 µm. (**C**) Capillary Western-blot analysis of dystrophin with the antibody DYSB and its quantification in the Dup2, Dup2–9, Dup8-9 and Dup2 clone 7, Dup2–9 clone 14, Dup8-9 clone 12 cell lines and C25 (positive control). The normalized signal corresponds to the ratio between the sample signal and the total protein signal of the same well. Three biological replicates were shown. A 2D representation of the capillary data is presented in Fig. S8B.

Target	Guide sequence + PAM	MIT specificity score	CFD Spec. score	Predicted efficiency score		Off-targets for 0–1–2–3–4 mismatches
				Doench'16	Mor-Mateos	
Dup2 + Dup2–9 (sgRNA1)	5′-GCATCTACATACTCTAAC AT-3′ In intron1	81	93	61	35	0–0–0–5–84
Dup2 + Dup2–9 (sgRNA 2)	5′-GTCAAACATGCATACTAT GT-3′ In intron2	81	89	41	36	0–0–3– 8–96
Dup2 + Dup2–9 (sgRNA3)	5′-GTCAAGATCTCAGTAACA CT-3′ In intron2	80	91	63	35	0–0–3– 8–96
Dup8-9 (sgRNA A)	5′-GTCAGATCAACTTAATGT GC-3′ In intron7	87	92	52	30	0–0–1–15–96
Dup8-9 (sgRNA B)	5′-AGCTGCAAACTTTGTGTT CG-3′ In intron9	84	91	32	18	0–0–0–6–58

Table 1. List of gRNAs designed with CRISPOR used in this article. Predicted specificity scores, efficiencies, outcomes and off-targets are indicated. Selected guides are in underline.

the distance between different cells can be larger than the distance between the corrected and uncorrected cells (Fig. S6B). Moreover, both our data and the GSE262976 dataset showed that corrected cells could be further away from WT cells. Altogether, these data indicated that comparison between non isogenic cells will not provide a correct assessment of the correction of the molecular pathway related to the disease.

Considering this point, for assessment of the molecular correction, we compared the dysregulated genes between the DMD duplication cells and their isogenic corrected clones and identified the dysregulated genes common to all three lines (Fig. 3C). Of these dysregulated genes, 43 were commonly down-regulated, and 21 were consistently up-regulated in all three corrected differentiated myogenic derivatives (Fig. 3C, Tables 2, 3, Supplemental excel file 2). Gene Ontology (GO) analysis revealed that these commonly dysregulated genes were enriched in three clusters: one related to actin filament, one related to response to potassium ion, and another related to muscle function (Fig. 3D, Supplemental excel file 3). All of these pathways are indeed related to deficiency in DMD[26–29]. Heat maps showing how the expression of this particular set of genes is modulated after duplication removal are presented in Fig. 3E.

Off target analysis

CRISPOR predicted no off-target sites with 1 or 2 mismatches (Supplemental excel file 4). Specific primers were designed for the twelve predicted off-target sites with 3 and 4 mismatches directly affecting exons (Table S3A). PCR amplifications were obtained for all sites in the edited clones (Fig. S7A–C) and Sanger sequencing revealed the absence of single nucleotide polymorphisms, insertions or deletions (indels) in any of them. A similar analysis was performed on six additional predicted off target sites located in the vicinity of genes shown to be dysregulated in the RNA-seq analysis (Table S3B). No sign of editing was found for any of them (Fig. S7D).

Discussion

The rapid development of the CRISPR/Cas9 gene editing tool has emerged as a promising avenue for treating a range of genetic diseases, with DMD standing out as a particularly compelling candidate[30–32]. Notably, this technique presents a unique opportunity for restoring the dystrophin reading frame. This can be achieved by utilizing two gRNAs that target different introns, facilitating the deletion of the exons in between without the concern of frameshift mutations caused by indels. The deletion of exons 45–55, for instance, employing a pair of gRNAs, holds the potential to correct up to 62% of DMD mutations, offering a versatile strategy applicable to a broad spectrum of cases[33,34].

Exon duplications, accounting for 10–15% of all DMD mutations offer the opportunity to restore the full reading frame of the *DMD* gene. By precisely targeting the duplicated region, a single guide RNA can execute two cuts, resulting in the deletion of the duplicated segment and the restoration of a full-length protein. The advantage of single sgRNA approach is that, theoretically, it offers higher gene editing efficiency, given the generally low in vivo efficiency of CRISPR cargo delivery (even lower for co-delivery), and a reduced probability of off-target effects[35,36]. Employing two sgRNAs may also lead to a higher probability of off-target incidents in comparison[37]. Since 2016, we and other groups demonstrated successful CRISPR-Cas9 mediated gene editing by employing a single guide RNA to delete different duplications[16–21]. Building upon these achievements, our current study extends this strategy to three distinct duplications, including the exon 2–9 duplication (to date the largest corrected by CRISPR spanning about 507 kb) and the exon 8–9 duplication (to date the smallest edited measuring 60 kb).

Through analysis of patient samples utilizing CGH analysis, we identified the minimal duplicated segments shared across the duplications reported in this article (Fig. S1). This crucial insight guided the design of our gRNA sequences, ensuring a highly specific and efficient approach while carefully avoiding splicing signals. Remarkably, this strategy successfully corrected duplications in all tested patient cells, as confirmed through ddPCR analysis using myoblast cells, immunostaining, and capillary western blotting with myotubes derived from these cells.

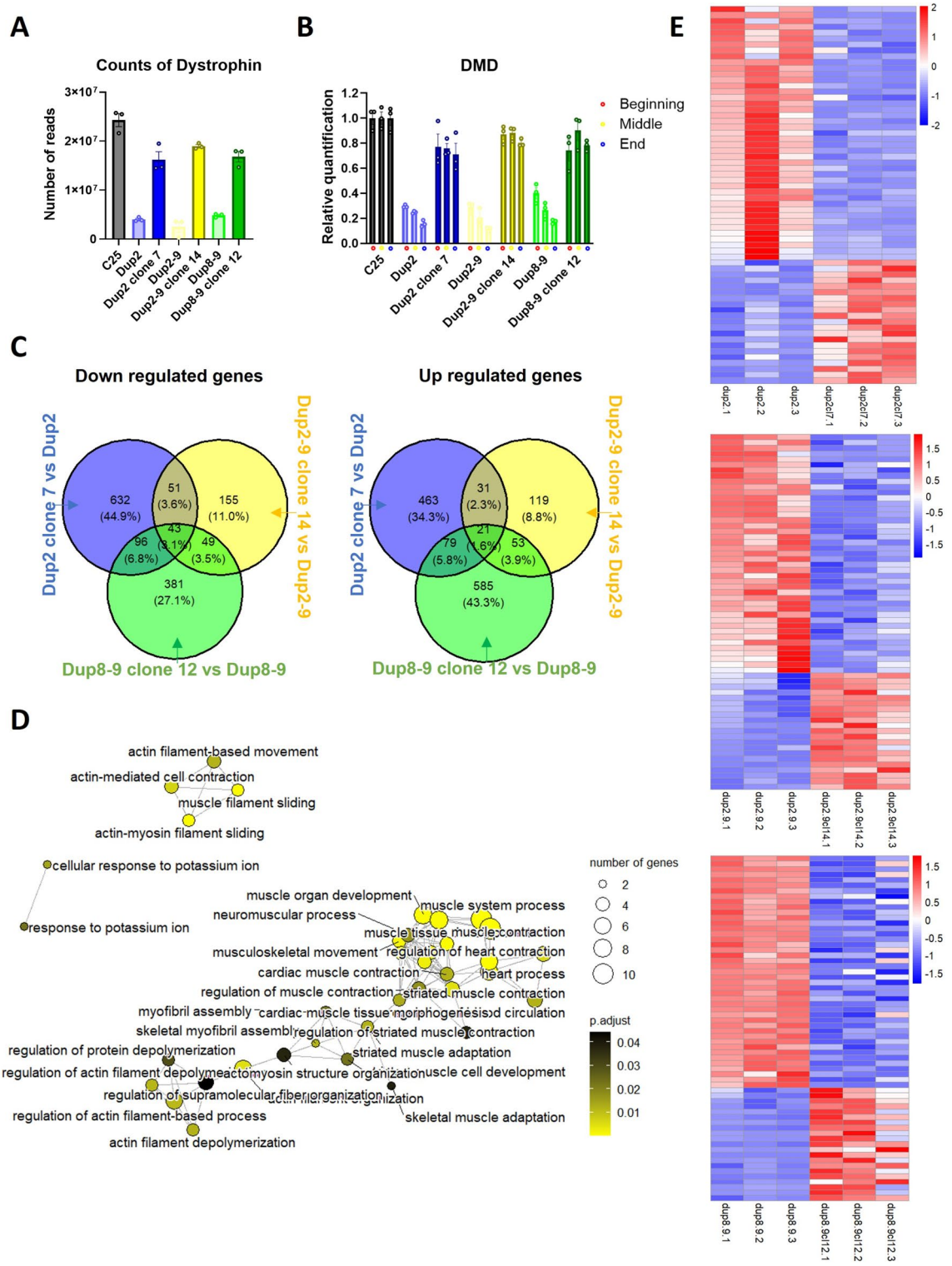

Figure 3. Correction of the DMD gene leads to its restored expression and the transcriptome profile of DMD disease. (**A**) Comparative level of dystrophin expression in the cell lines before and after gene editing as indicated by RNA-seq read counts. (**B**) The related exon counts of DMD. The DMD exons were divided into Beginning, Middle, and End exons. (**C**) Venn diagrams showing the overlap of modified genes in common between the different cell lines. The comparison between Dup2 and Dup2 clone 7 is in blue. between Dup2–9 and Dup2–9 clone 14 in yellow between Dup8-9 and Dup8-9 clone 12 in green. (**D**) Pathway networks of Gene Ontology (GO) analysis of the commonly dysregulated genes. Three clusters were identified: one related to actin filament, one related to actin filament, one related to response to potassium ion and another related to muscle function. (**E**) Heatmap visualization of the expression of the 43 commonly down-regulated and 21 up-regulated genes in the uncorrected and corrected cells.

	Dup2 clone 7 vs Dup2		Dup2–9 clone 14 vs Dup2–9		Dup8-9 clone 12 vs Dup8-9	
Name	Fold change (Log_2)	p-value	Fold change (Log_2)	p-value	Fold change (Log_2)	p-value
MAN1C1	0.84	0.004762	0.74	0.000139	0.61	0.049479
NEGR1	1.25	1.69E−13	1.30	1.98E−28	0.98	1.07E−13
MAPK10	1.12	1.56E−07	0.65	0.000104	1.73	8.29E−06
RNF150	0.68	0.013628	1.07	4.67E−15	2.28	3.15E−09
PTCHD4	0.92	0.000939	0.58	0.002661	0.67	0.002589
COL19A1	0.90	5.44E−08	1.09	1.39E−34	3.04	4.97E−06
BAIAP2L1	2.27	1.09E−27	1.39	4.57E−16	1.59	6.61E−05
MSR1	1.25	0.005971	1.10	6.42E−10	1.10	4.05E−05
LINC01239	1.10	5.03E−05	0.85	0.000106	1.60	0.000413
RTKN2	1.29	6.31E−09	0.75	8.44E−05	2.36	4.02E−15
DNMBP	1.00	1.03E−14	0.52	0.001605	1.39	7.59E−18
CDKN1C	0.99	1.45E−05	0.69	8.76E−08	1.60	3.44E−08
ARHGAP20	1.23	3.37E−09	0.81	3.63E−08	1.00	2.54E−05
METTL7A	1.03	0.001604	0.78	0.000394	1.47	0.000928
SLITRK5	1.90	8.22E−19	0.78	5.90E−07	1.98	1.07E−22
ADGRG1	0.95	2.72E−05	0.70	1.67E−10	1.98	0.000683
HSD11B2	1.32	9.62E−14	0.91	1.59E−10	1.35	1.82E−05
ABCA8	1.41	2.59E−13	0.68	1.70E−05	0.53	0.001833
NOL4L	0.91	0.005077	0.53	0.041591	1.29	2.30E−07
KREMEN1	1.26	2.45E−07	0.59	9.99E−08	0.84	4.43E−07
DMD	2.02	3.82E−37	2.47	6.40E−200	1.78	7.68E−41

Table 2. List of the up-regulated genes in common in all the edited clones versus the parental line. Fold changes (Log_2) and adjusted p-value are indicated.

The quantitative and immunofluorescence staining of clones corrected via sgRNA CRISPR strategy underlines the efficacy of the single guide approach for the correction of large as well as small duplicated DNA region on *DMD* gene. In fact, the same gRNA was used to target two duplications of different sizes (a 157 kb duplication of exon 2 and a 507 kb duplication of exons 2–9) obtaining more corrected clones (Fig. 2A) and a higher amount of restored dystrophin (Fig. 2B) from the cells with the larger duplication. This could imply that factors beyond the size of the duplication such as chromatin structure may influence the efficiency of correction.

One aspect worth mentioning is that, despite the successful deletion of the *DMD* duplication regions, the resulting cell lines only express approximately 20% of dystrophin at protein levels compared to the WT C25 differentiated myotube. One possibility is that although we have successfully corrected the *DMD* gene, the chromatin status may not have been fully reversed[38]. It is conceivable that the cells may require more time and/or additional chromatin remodeling factors to erase the epigenetic memories. Specifically, it has been reported that Histone 3 lysine 9 trimethylation (H3K9me3) levels at the exons of DMD were increased in mdx mice compared to WT, along with elevated expression levels of the histone methyltransferases[39]. Other possibilities include the inefficiency of DMD protein translation and the instability of DMD protein related to insufficient level of intervening proteins due to incomplete differentiation process. Studying the mechanisms of the lower DMD protein expression level after DMD correction would be our next step for enhancing the efficacy of *DMD* gene editings.

Additionally, we demonstrated that this correction also restores the expression of genes impacted by DMD, as evidenced by RNA-seq data. However, in our study, we only have one WT myoblast cell line, which is not isogenic or coming from family members of any of the three DMD duplication cells. This is one limitation of our study. Indeed, the differences in the transcriptomic profiles between the WT C25 and the three DMD duplication cells may arise from the absence of the DMD protein or from other differences in the cell background as it was reported in other cases[36,40,41]. Analysis of the data from another study that used a similar transcriptomics profiling technique confirmed that comparison between non isogenic cells will not provide a correct molecular assessment of the correction[25].

Intriguingly, both in our data and the dataset from the literature[25], the DMD corrected cells could be further away from WT cells compared to uncorrected cells, possibly with an increase distance in correlation with the level of the restored DMD transcript. This effect may reflect an complex interplay between the cell fitness and the level of normal or aberrant DMD transcripts.

Another limitation of this study is that the experiments were performed in vitro. On one hand, there is an advantage to using human cells since the gene editing tools will specifically be appropriate for the human genome. On the other hand, it is possible that the efficacy of editing will differ between the in vitro and the in vivo situations. It was, in fact, previously reported that gene editing efficacy and mechanisms differ according to chromatin accessibility and cell cycle status[42–44]. To address this issue, we are currently constructing a humanized mouse model for one of the duplications. We will further evaluate our single gRNA strategy in vivo with this model.

	Dup2 clone 7 vs Dup2		Dup2–9 clone 14 vs Dup2–9		Dup8-9 clone 12 vs Dup8-9	
Name	Fold change (Log_2)	p-value	Fold change (Log_2)	p-value	Fold change (Log_2)	p-value
SLC2A5	−1.79	0.041072	−0.86	0.016686	−2.28	1.28E−09
TCEA3	−2.26	4.07E−26	−1.98	1.11E−13	−2.71	0.000303
CYP2J2	−2.23	2.86E−13	−0.67	0.005583	−1.87	0.04932
COLGALT2	−0.53	0.029801	−0.56	0.024238	−0.90	0.040629
ACTA1	−1.23	1.60E−07	−0.72	3.13E−07	−0.83	2.25E−10
ACTN2	−0.98	0.00018	−0.87	6.88E−18	−1.26	6.59E−31
MAPRE3	−1.18	1.69E−41	−0.53	0.001313	−0.65	0.011501
XIRP1	−0.53	0.009874	−0.62	2.56E−06	−1.03	3.75E−11
DOCK3	−0.81	0.000267	−0.87	0.007964	−1.70	1.85E−08
TWF2	−0.69	0.003275	−0.73	8.25E−05	−0.86	3.25E−07
TNNC1	−1.55	5.70E−08	−0.69	2.77E−05	−1.74	0.00287
MYLK	−1.32	1.80E−05	−0.59	2.36E−09	−0.63	6.03E−05
TFRC	−0.59	0.007892	−1.77	3.46E−06	−0.85	0.013466
DDIT4L	−0.78	0.001823	−1.21	0.002426	−1.37	0.000936
PROB1	−1.18	7.31E−09	−1.17	1.31E−13	−1.41	0.049479
SH2B2	−0.59	0.000206	−0.59	0.002619	−0.93	5.85E−08
PRRT4	−0.94	0.001442	−0.86	0.006096	−0.68	0.010975
AQP3	−0.87	0.000163	−0.83	3.14E−07	−0.85	0.000175
PYGM	−1.67	0.026204	−1.56	4.34E−25	−1.62	5.42E−21
PPME1	−0.82	4.12E−08	−0.73	2.45E−06	−0.58	4.86E−09
DLG2	−1.67	1.08E−12	−2.97	6.04E−59	−1.40	3.12E−06
TSPAN9	−1.20	1.05E−23	−1.19	3.49E−21	−1.07	1.59E−22
NR4A1	−0.94	6.79E−07	−0.56	0.037923	−1.24	1.31E−06
MYL6B	−0.85	2.28E−07	−1.06	1.95E−12	−1.24	5.10E−09
SPTB	−2.05	1.34E−14	−1.30	8.72E−16	−1.19	0.000381
TGFB3	−0.84	9.26E−05	−0.62	8.44E−05	−1.08	7.81E−14
DNAJA4	−1.52	8.05E−05	−1.02	4.15E−08	−1.76	1.77E−20
AGBL1	−0.91	0.024366	−1.47	2.48E−11	−1.98	5.17E−09
CACNA1H	−1.46	6.06E−07	−2.53	1.39E−20	−4.14	8.81E−08
GPT2	−0.83	5.03E−06	−0.60	0.000647	−1.20	4.00E−12
MYH2	−0.83	0.002875	−0.71	4.95E−06	−1.20	2.13E−07
KCNJ12	−1.85	1.23E−17	−1.59	1.95E−06	−1.46	0.005151
TCAP	−1.74	2.62E−09	−1.09	7.97E−05	−2.49	2.20E−14
JUP	−3.69	6.54E−18	−1.68	2.97E−07	−2.97	6.11E−60
ENSG00000289579	−0.73	0.005741	−0.85	0.000567	−0.92	0.0357
ST8SIA5	−2.45	3.93E−19	−1.05	0.001069	−1.67	1.08E−10
RNF152	−0.68	0.001255	−0.93	1.67E−06	−0.93	0.027516
DIRAS1	−1.35	8.21E−23	−1.40	5.15E−16	−1.46	5.54E−11
PRDX2	−3.37	1.02E−37	−0.81	2.23E−07	−0.52	0.000334
WDR62	−0.94	0.010375	−0.59	0.023525	−0.92	0.009013
EEF1A2	−1.87	1.32E−31	−0.73	7.05E−06	−0.93	0.000216
CSDC2	−1.17	0.016286	−0.59	0.011969	−1.04	2.96E−11
XG	−1.38	1.52E−15	−1.26	0.000209	−1.17	0.03654

Table 3. List of the down-regulated genes in common in all the edited clones versus the parental line. Fold changes (Log_2) and adjusted p-value are indicated.

By validating the feasibility of targeting and correcting duplication events using a sgRNA, we have demonstrated the low toxicity of our approach by analyzing off-target regions either predicted in exonic region and in regions close to dysregulated genes identified by RNAseq. In conclusion, our study extends the application of the CRISPR/Cas9 system to new *DMD* gene duplications, thereby contributing to an expanded understanding of the safety profile of this editing strategy. Through specific target identification and gRNA design, we have successfully demonstrated the feasibility of restoring gene expression and protein functionality. These findings provide a blueprint for addressing a wider range of genetic disorders stemming from tandem duplications.

Material and methods

Patients' cells

The Biobank of Cells, tissues and DNA from patients with neuromuscular diseases, member of the Telethon Network of Genetic Biobanks (project no. GTB12001), funded by Telethon Italy, and of the EuroBioBank network, provided us with myoblasts from patients with exon 2–9 and 8-9 duplications. Myoblasts from a patient with exon 2 duplication were previously obtained[17]. These cells were transferred to the Myoline platform of the Institute of and immortalized as previously described[45]. The immortalized myoblasts C25 was generated from a healthy male and provided by the Myoline[46]. Informed consent was obtained from all patients to conduct the study, in accordance with the Helsinki Declaration. All the experimental procedures were approved by Genethon.

Immortalized myoblasts were maintained and cultured at 37 °C and 5% CO_2 in Skeletal Muscle Cell Growth Medium supplemented with Supplement Mix solution (Promocell) and gentamycin (10 µg/mL). Additionally, the medium was supplemented with 15% FCS, 1% GlutaMAX (Thermo Scientific), and 1% gentamicin (Life technologies). To induce differentiation, the culture medium was replaced with differentiation medium (Promocell) supplemented with recombinant human insulin at 10 µg/mL and gentamycin (10 µg/mL) when the myoblasts reach 80% confluence.

Characterization of duplications by CGH and digital droplet PCR

DNA was extracted from cells using the DNeasy Blood and Tissue kit (Qiagen). Samples were then quantified by Nanodrop (NanoDrop™ 8000) and stored at – 20 °C.

Comparative genomic hybridization (CGH) analysis by DMD-CGH microarray was performed as previously described[22].

For ddPCR, DNA samples were fractioned into droplets suspended in oil with Biorad AutoDG machine. After the droplet generation (AutoDG Droplet, BioRad), extracted DNA (10 ng) was used with the following PCR amplification conditions: initial denaturation at 95 °C for 10 min, followed by 44 cycles of denaturation at 94 °C for 30 s, annealing and extension at 54 °C for 1 min. Then, fluorescent dye stabilization was performed at 98 °C for 10 min. Multiplex channels were then analyzed by QX Manager 1.2 Standard Edition software (QX200, BioRad). Primers and probes used are referenced in Table S1. The analysis was performed using the Quantasoft analysis pro software and was calculated as copies of DNA.

CRISPR in-tube

The sgRNA design was performed with CRISPOR software[23] (http://crispor.tefor.net/). The best predicted sequences were synthetized (Sigma; Table 1) and used to generate RNA using the EnGen 2X sgRNA Reaction Mix, 0.1 M DTT, and the EnGen sgRNA Enzyme Mix (EnGen® sgRNA synthesis kit, S. pyogenes; NEB). The gRNAs were mixed with SpCas9 nuclease to generated RNP complexes. The DMD target loci were PCR amplified and quantified using Nanodrop with the primers shown in Table S2. Three nM of PCR product were mixed with the RNP complex (30 nM of gRNA and 30 nM SpCas9) and left for cleavage for 15 min at 37 °C. The resulting products were then loaded for chip-based bioanalysis using the Agilent 206 Bioanalyzer (Agilent) and the cleavage was calculated using the following estimation: % modification = 100 × ([uncut DNA]/[uncut DNA] + [fragment1] + [fragment2]).

HEK293 culture and transfection

The 20 bp guide sequences targeting Dup8-9 duplication (Table 1) were cloned into a SpCas9-2A-GFP vector (px458 was a gift from Feng Zhang, Addgene plasmid # 48138). Plasmid DNA was prepared by following the protocol of NucleoBond PC 500 kit (Macherey–Nagel). HEK293T cells were cultured in Dulbecco's Modified Eagle Medium (DMEM) GlutaMAX (ThermoFisher Scientific) supplemented with 10% fetal bovine serum (FCS) (Eurobio) and gentamicin (10 µg/mL; ThermoFisher Scientific) at 37 °C with a 5% CO2. At 80% confluency, they were transfected with 2 µg of DNA of px458 plasmids containing the Cas9, the target sgRNA and control px458 plasmid with no sgRNA using the Lipofectamine 2000 reagent (ThermoFisher Scientific). After 2 days, GFP fluorescence was visualized by Evos microscope (ThermoFisher) and after 5 days, DNA was extracted, regions of interest are amplified by PCR. PCR products were deposited on agarose gel, and bands were sequenced and analysed on TIDE (https://tide.nki.nl/).

Nucleofection of immortalized myogenic cell lines and cell sorting

The P5 Primary Cell 4D-NucleofectorTM X Kit S (Lonza) was used for the nucleofection of immortalized myoblasts. The sgRNAs and Cas9 protein (20 pmol of Cas9 protein for 90 pmol of guide RNA at 100 nM) were mixed with the nucleofection solution, incubated for 10 min at room temperature (RT), and then kept on ice. The cells were dissociated with TrypLE® Express 1X enzyme (ThermoFisher Scientific), pelleted and resuspended in the nucleofection solution to achieve a cell concentration of 150,000 cells/well, and mixed with the solution containing the RNP complex in a well. Nucleofection was carried out using the CM-138 program on the Amaxa™ 4D-Nucleofector™ device (Lonza). Subsequently, the nucleofected cells were seeded in a 6-well plate, and cultured for 2 days before sorting. The nucleofected Dup2, Dup2–9 and Dup8-9 cells were dissociated using TrypLE® Express 1X enzyme and resuspended in pre-warmed medium. Sorting was performed on the flow cytometer CytoFLEX (Beckman Coulter Life Sciences) or the cell sorter ASTRIOS-EQ (Beckman Coulter Life Sciences) to sort one cell per well in a 96-well plate containing the Skeletal Muscle Cell Growth Medium (Promocell) medium.

Immunostaining

Cells were seeded in ibiTreat µ-Dish 35 mm high culture dishes (Ibidi) until confluence and differentiation. Cells were rinsed with phosphate buffer saline (PBS) and fixed with 4% formaldehyde solution (PFA) for 30 min at RT. After one PBS wash, the blocking solution, composed of 10% goat serum at 10% (v/v in PBS) was added for 45 min at RT. Cells were incubated with 1:50 anti-dystrophin primary antibody (Leica: NCL-DYSB) and 1:100 anti-alpha-actinin2 primary antibody (Invitrogen) diluted with PBS in 10% blocking buffer overnight at 4 °C (Table S4A). Cells were washed three times in PBS and incubated for 45 min at RT with Alexa-conjugated secondary antibodies (Goat anti-mouse Alexa fluor 594, Life Technologies, and Goat anti-rabbit Alexa fluor 594), 1:1000 in 10% blocking solution at a dark humid chamber (Table S4B). Samples were washed three times in PBS and mounted in DAPI Fluoromount-G (Southern Biotech, Birmingham, AL, USA. Images were digitalized using Axioscan Z1 slide scanner (Zeiss, Jena, Germany).

Dystrophin quantification

Amount of produced full-length dystrophin was assessed by the Jess™ Simple Western Automated Immunoassay System (ProteinSimple, San Jose, CA, USA™, Bio-Techne brand). Mechanically disrupted samples were processed according to the manufacturer's standard method for the Jess 66–440-kDa Separation Module (SM-W008). Briefly, a mixture of samples, fluorescent molecular weight marker and 400 mM dithiothreitol (ProteinSimple) was prepared at a final concentration of 0.25 µg/µl. The mixture was denatured at 95 °C for 5 min. The migration of the proteins through the separation matrix was done at 375 V. The separated proteins were incubated with an anti-mouse HRP-conjugated IgG antibodies (corresponding to the species of the antibody used, DysB). Peroxide/Luminol-S (ProteinSimple) was used for chemiluminescent revelation.

RNA-seq analysis

Total RNA extraction was performed from myotubes (at day 8 of differentiation) lysates using the RNeasy Plus kit (Qiagen). Total RNA concentration was quantified using a Nanodrop spectrophotometer (ND8000 Labtech, Wilmington Delaware). The RNA quality was evaluated using an Agilent RNA 6000 Pico Kit on a 2100 Bioanalyzer instrument (Agilent Technologies) and Illumina RNA seq was performed on three replicates of each selected clone. The sequencing libraries were prepared using the TruSeq Stranded Total RNA Library Prep Kit (Illumina) and sequenced according to the Illumina NovaSeq™ 6000 protocol. Paired-end reads (2 × 150 bp) were aligned on the reference transcriptome (GRCh38.p13/GENECODE release 43) using STAR version 2.7.11b[47], after excluding samples showing at the same time a low number of reads and a low percentage of alignment. Gene expression was measured by featureCounts version 2.0.6. Quantification files were processed using R (4.4.0) to perform differential expression analysis. Pairwise group differential expression were performed using DESeq2 (1.40.1) considering genes with more than 100 reads in at least three samples (lfcThreshold = 0, pAdjustMethod = "fdr", independentFiltering = T). Genes were considered dysregulated if the absolute Log fold change was above 0.5 and the FDR adjusted p.value below 0.05.

Detection of indels in off-targets sites

Primers flanking off-target sites of respective sgRNAs were designed when corresponding to exonic regions (Table S3A). Similarly, primers flanking intronic/intergenic off target sites with highest Cutting Frequency Determination (CFD) off-target score (Haeussler et al. 2016)[48] and found dysregulated in the RNAseq analysis were designed (Table S3B). The genomic DNA from the DMD mutant Dup2, Dup2–9 and Dup8-9 along with corrected Dup2 clone 7, Dup2–9 clone 14 and Dup 8-9 clone 12 were isolated using DNeasy Blood and Tissue kit (Qiagen) after 8 days of differentiation. Off target sites were PCR amplified, with Q5® High-Fidelity DNA Polymerase (New England Biolabs, M0492S) from the genomic DNA isolated from mutant and edited cells. PCR products were run on agarose (Eurobio Scientific, GEPAGA07-65) gel and remaining PCR products were Sanger sequenced. The sequencing results were analyzed using TIDE analysis software[49] (https://tide.nki.nl/) to identify potential off-target effects of CRISPR editing.

Statistical analysis

GraphPad Prism 8 was used to calculate the mean and standard deviation of the data. For R (4.4.0), the tximport package (1.28.0) was used. GSEA were performed using the reactomePA (1.44.0) and clusterProfiler (4.8.1) packages for reactome and GO terms. All the experiments were repeated at least three times with independent biological replicates. The data shown represent mean ± SEM from the three independent experiments.

Data availability

The RNA-seq data generated in this study have been deposited in the NCBI Gene Expression Omnibus (GEO) database under accession number GSE272233. All the other data associated with this study are shown in the manuscript and supplementary information.

Received: 30 January 2024; Accepted: 12 August 2024
Published online: 11 September 2024

References

1. Hoffman, E. P., Brown, R. H. Jr. & Kunkel, L. M. Dystrophin: The protein product of the Duchenne muscular dystrophy locus. *Cell* **51**, 919–928. https://doi.org/10.1016/0092-8674(87)90579-4 (1987).
2. Mercuri, E., Bonnemann, C. G. & Muntoni, F. Muscular dystrophies. *Lancet* **394**, 2025–2038. https://doi.org/10.1016/S0140-6736(19)32910-1 (2019).

3. Monaco, A. P. *et al.* Isolation of candidate cDNAs for portions of the Duchenne muscular dystrophy gene. *Nature* **323**, 646–650. https://doi.org/10.1038/323646a0 (1986).
4. Beggs, A. H., Koenig, M., Boyce, F. M. & Kunkel, L. M. Detection of 98% of DMD/BMD gene deletions by polymerase chain reaction. *Hum. Genet.* **86**, 45–48. https://doi.org/10.1007/BF00205170 (1990).
5. Babbs, A. *et al.* From diagnosis to therapy in Duchenne muscular dystrophy. *Biochem. Soc. Trans.* **48**, 813–821. https://doi.org/10.1042/BST20190282 (2020).
6. Wilton-Clark, H. & Yokota, T. Antisense and gene therapy options for duchenne muscular dystrophy arising from mutations in the N-terminal hotspot. *Genes (Basel).* https://doi.org/10.3390/genes13020257 (2022).
7. Wasala, N. *et al.* Life-long outcomes of systemic AAV micro-dystrophin gene therapy in a murine Duchenne muscular dystrophy model. *Hum. Gene Ther.* https://doi.org/10.1089/hum.2022.181 (2022).
8. Boehler, J. F. *et al.* Clinical potential of microdystrophin as a surrogate endpoint. *Neuromuscul. Disord.* https://doi.org/10.1016/j.nmd.2022.12.007 (2022).
9. Birch, S. M. *et al.* Assessment of systemic AAV-microdystrophin gene therapy in the GRMD model of Duchenne muscular dystrophy. *Sci. Transl. Med.* **15**, eabo1815. https://doi.org/10.1126/scitranslmed.abo1815 (2023).
10. Yu, A. M. & Tu, M. J. Deliver the promise: RNAs as a new class of molecular entities for therapy and vaccination. *Pharmacol. Ther.* **230**, 107967. https://doi.org/10.1016/j.pharmthera.2021.107967 (2022).
11. Hoy, S. M. Delandistrogene moxeparvovec: First approval. *Drugs* **83**, 1323–1329. https://doi.org/10.1007/s40265-023-01929-x (2023).
12. Heo, Y. A. Golodirsen: First approval. *Drugs* **80**, 329–333. https://doi.org/10.1007/s40265-020-01267-2 (2020).
13. Komaki, H. *et al.* Viltolarsen in Japanese Duchenne muscular dystrophy patients: A phase 1/2 study. *Ann. Clin. Transl. Neurol.* **7**, 2393–2408. https://doi.org/10.1002/acn3.51235 (2020).
14. Zakeri, S. E. *et al.* Casimersen for the treatment of Duchenne muscular dystrophy. *Trends Pharmacol. Sci.* **43**, 607–608. https://doi.org/10.1016/j.tips.2022.04.009 (2022).
15. Shen, W., Liu, S. & Ou, L. rAAV immunogenicity, toxicity, and durability in 255 clinical trials: A meta-analysis. *Front. Immunol.* **13**, 1001263. https://doi.org/10.3389/fimmu.2022.1001263 (2022).
16. Wojtal, D. *et al.* Spell checking nature: Versatility of CRISPR/Cas9 for developing treatments for inherited disorders. *Am. J. Hum. Genet.* **98**, 90–101. https://doi.org/10.1016/j.ajhg.2015.11.012 (2016).
17. Lattanzi, A. *et al.* Correction of the exon 2 duplication in DMD myoblasts by a single CRISPR/Cas9 system. *Mol. Ther. Nucleic Acids* **7**, 11–19. https://doi.org/10.1016/j.omtn.2017.02.004 (2017).
18. Long, C. *et al.* Correction of diverse muscular dystrophy mutations in human engineered heart muscle by single-site genome editing. *Sci. Adv.* **4**, eaa9004. https://doi.org/10.1126/sciadv.aap9004 (2018).
19. Wang, D. N., Wang, Z. Q., Jin, M., Lin, M. T. & Wang, N. CRISPR/Cas9-based genome editing for the modification of multiple duplications that cause Duchenne muscular dystrophy. *Gene Ther.* **29**, 730–737. https://doi.org/10.1038/s41434-022-00336-3 (2022).
20. Pini, V. *et al.* Transiently expressed CRISPR/Cas9 induces wild-type dystrophin in vitro in DMD patient myoblasts carrying duplications. *Sci. Rep.* **12**, 3756. https://doi.org/10.1038/s41598-022-07671-w (2022).
21. Maino, E. *et al.* Targeted genome editing in vivo corrects a Dmd duplication restoring wild-type dystrophin expression. *EMBO Mol. Med.* **13**, e13228. https://doi.org/10.15252/emmm.202013228 (2021).
22. Bovolenta, M. *et al.* A novel custom high density-comparative genomic hybridization array detects common rearrangements as well as deep intronic mutations in dystrophinopathies. *BMC Genom.* **9**, 572. https://doi.org/10.1186/1471-2164-9-572 (2008).
23. Concordet, J. P. & Haeussler, M. CRISPOR: Intuitive guide selection for CRISPR/Cas9 genome editing experiments and screens. *Nucleic Acids Res.* **46**, W242–W245. https://doi.org/10.1093/nar/gky354 (2018).
24. Ran, F. A. *et al.* Genome engineering using the CRISPR-Cas9 system. *Nat. Protoc.* **8**, 2281–2308. https://doi.org/10.1038/nprot.2013.143 (2013).
25. Dhoke, N. R. *et al.* A novel CRISPR-Cas9 strategy to target DYSTROPHIN mutations downstream of exon 44 in patient-specific DMD iPSCs. *Cells.* https://doi.org/10.3390/cells13110972 (2024).
26. Kornegay, J. N. *et al.* The paradox of muscle hypertrophy in muscular dystrophy. *Phys. Med. Rehabil. Clin. N. Am.* **23**, 149–172, xii. https://doi.org/10.1016/j.pmr.2011.11.014 (2012).
27. Faber, R. M., Hall, J. K., Chamberlain, J. S. & Banks, G. B. Myofiber branching rather than myofiber hyperplasia contributes to muscle hypertrophy in mdx mice. *Skelet. Muscle* **4**, 10. https://doi.org/10.1186/2044-5040-4-10 (2014).
28. Massopust, R. T. *et al.* Lifetime analysis of mdx skeletal muscle reveals a progressive pathology that leads to myofiber loss. *Sci. Rep.* **10**, 17248. https://doi.org/10.1038/s41598-020-74192-9 (2020).
29. Dubinin, M. V. & Belosludtsev, K. N. Ion channels of the sarcolemma and intracellular organelles in duchenne muscular dystrophy: A role in the dysregulation of ion homeostasis and a possible target for therapy. *Int. J. Mol. Sci.* https://doi.org/10.3390/ijms24032229 (2023).
30. Asher, D. R. *et al.* Clinical development on the frontier: Gene therapy for duchenne muscular dystrophy. *Expert Opin. Biol. Ther.* **20**, 263–274. https://doi.org/10.1080/14712598.2020.1725469 (2020).
31. Gupta, S., Sharma, S. N., Kundu, J., Pattanayak, S. & Sinha, S. Morpholino oligonucleotide-mediated exon skipping for DMD treatment: Past insights, present challenges and future perspectives. *J. Biosci.* **48** (2023).
32. Li, T. *et al.* CRISPR/Cas9 therapeutics: Progress and prospects. *Signal Transduct. Target Ther.* **8**, 36. https://doi.org/10.1038/s41392-023-01309-7 (2023).
33. Young, C. S. *et al.* A single CRISPR-Cas9 deletion strategy that targets the majority of DMD patients restores dystrophin function in hiPSC-derived muscle cells. *Cell Stem Cell* **18**, 533–540. https://doi.org/10.1016/j.stem.2016.01.021 (2016).
34. Ousterout, D. G. *et al.* Multiplex CRISPR/Cas9-based genome editing for correction of dystrophin mutations that cause Duchenne muscular dystrophy. *Nat. Commun.* **6**, 6244. https://doi.org/10.1038/ncomms7244 (2015).
35. Dabrowska, M. *et al.* qEva-CRISPR: A method for quantitative evaluation of CRISPR/Cas-mediated genome editing in target and off-target sites. *Nucleic Acids Res.* **46**, e101. https://doi.org/10.1093/nar/gky505 (2018).
36. Gillmore, J. D. *et al.* CRISPR-Cas9 in vivo gene editing for transthyretin amyloidosis. *N. Engl. J. Med.* **385**, 493–502. https://doi.org/10.1056/NEJMoa2107454 (2021).
37. Haeussler, M. CRISPR off-targets: A question of context. *Cell Biol. Toxicol.* **36**, 5–9. https://doi.org/10.1007/s10565-019-09497-1 (2020).
38. Bizot, F. *et al.* Histone deacetylase inhibitors improve antisense-mediated exon-skipping efficacy in mdx mice. *Mol. Ther. Nucleic Acids* **30**, 606–620. https://doi.org/10.1016/j.omtn.2022.11.017 (2022).
39. Garcia-Rodriguez, R. *et al.* Premature termination codons in the DMD gene cause reduced local mRNA synthesis. *Proc. Natl. Acad. Sci. USA* **117**, 16456–16464. https://doi.org/10.1073/pnas.1910456117 (2020).
40. Kilpinen, H. *et al.* Common genetic variation drives molecular heterogeneity in human iPSCs. *Nature* **546**, 370–375. https://doi.org/10.1038/nature22403 (2017).
41. Miura, K. *et al.* Variation in the safety of induced pluripotent stem cell lines. *Nat. Biotechnol.* **27**, 743–745. https://doi.org/10.1038/nbt.1554 (2009).
42. Uusi-Makela, M. I. E. *et al.* Chromatin accessibility is associated with CRISPR-Cas9 efficiency in the zebrafish (Danio rerio). *PLoS One* **13**, e0196238. https://doi.org/10.1371/journal.pone.0196238 (2018).

43. Ito, Y. *et al.* Epigenetic profiles guide improved CRISPR/Cas9-mediated gene knockout in human T cells. *Nucleic Acids Res.* **52**, 141–153. https://doi.org/10.1093/nar/gkad1076 (2024).
44. Shin, J. J. *et al.* Controlled cycling and quiescence enables efficient HDR in engraftment-enriched adult hematopoietic stem and progenitor cells. *Cell Rep.* **32**, 108093. https://doi.org/10.1016/j.celrep.2020.108093 (2020).
45. Mamchaoui, K. *et al.* Immortalized pathological human myoblasts: Towards a universal tool for the study of neuromuscular disorders. *Skelet. Muscle* **1**, 34. https://doi.org/10.1186/2044-5040-1-34 (2011).
46. Thorley, M. *et al.* Skeletal muscle characteristics are preserved in hTERT/cdk4 human myogenic cell lines. *Skelet. Muscle* **6**, 43. https://doi.org/10.1186/s13395-016-0115-5 (2016).
47. Dobin, A. *et al.* STAR: Ultrafast universal RNA-seq aligner. *Bioinformatics* **29**, 15–21. https://doi.org/10.1093/bioinformatics/bts635 (2013).
48. Haeussler, M. *et al.* Evaluation of off-target and on-target scoring algorithms and integration into the guide RNA selection tool CRISPOR. *Genome Biol.* **17**(1), 148. https://doi.org/10.1186/s13059-016-1012-2 (2016).
49. Brinkman, E. K., Chen, T., Amendola, M. & van Steensel, B. Easy quantitative assessment of genome editing by sequence trace decomposition. *Nucleic Acids Res.* **42**, e168. https://doi.org/10.1093/nar/gku936 (2014).

Acknowledgements

We are grateful to the "Imaging and Cytometry Core Facility" of Genethon for technical support and to Ile-de-France Region, for the purchase of the equipment and to GIP Genopole, Evry, and INSERM for the purchase of the equipment. We thank the Myoline platform of the Institute of Myology (Paris, France) for immortalization of human cells and Marina Mora for providing us the specimens through the Biobank of Cells, tissues and DNA from patients with neuromuscular diseases, member of the Telethon network of Genetic Biobanks (Project number GTB12001), funded by Telethon Ital y and EuroBioBank network (www.eurobiobank.org). This work was supported by Grants from the Horinzon 2020 Marie Sklodowska-Curie Individual Fellowship Action (Project DMD2CURE #703093) to M.B and AFM-Téléthon (Project 3GEP).

Author contributions

J.L, A.Du, A.Do, A.J, M.B. and K.M. performed the experiments; G.C. performed computational analyses; M.B. and I.R. conceived the experiments; J.L., G.W., T.W. and A.Du. wrote the draft of the manuscript, M.B. and I.R. reviewed and edited the manuscript.

Competing interests

The authors declare no competing interests.

Additional information

Supplementary Information The online version contains supplementary material available at https://doi.org/10.1038/s41598-024-70075-5.

Correspondence and requests for materials should be addressed to I.R.

Reprints and permissions information is available at www.nature.com/reprints.

Publisher's note Springer Nature remains neutral with regard to jurisdictional claims in published maps and institutional affiliations.

Open Access This article is licensed under a Creative Commons Attribution-NonCommercial-NoDerivatives 4.0 International License, which permits any non-commercial use, sharing, distribution and reproduction in any medium or format, as long as you give appropriate credit to the original author(s) and the source, provide a link to the Creative Commons licence, and indicate if you modified the licensed material. You do not have permission under this licence to share adapted material derived from this article or parts of it. The images or other third party material in this article are included in the article's Creative Commons licence, unless indicated otherwise in a credit line to the material. If material is not included in the article's Creative Commons licence and your intended use is not permitted by statutory regulation or exceeds the permitted use, you will need to obtain permission directly from the copyright holder. To view a copy of this licence, visit http://creativecommons.org/licenses/by-nc-nd/4.0/.

© The Author(s) 2024